Supporting Information

A general strategy towards carbon nanosheets from triblock polymer for high-rate anode material in lithium and sodium ion batteries

Yaxin Chen, Liluo Shi, Shasha Guo, Qiong Yuan, Xiaohong Chen, Jisheng Zhou and Huaihe Song*

State Key Laboratory of Chemical Resource Engineering, Beijing Key Laboratory of Electrochemical Process and Technology for Materials, Beijing University of Chemical Technology, Beijing 100029, P. R. China

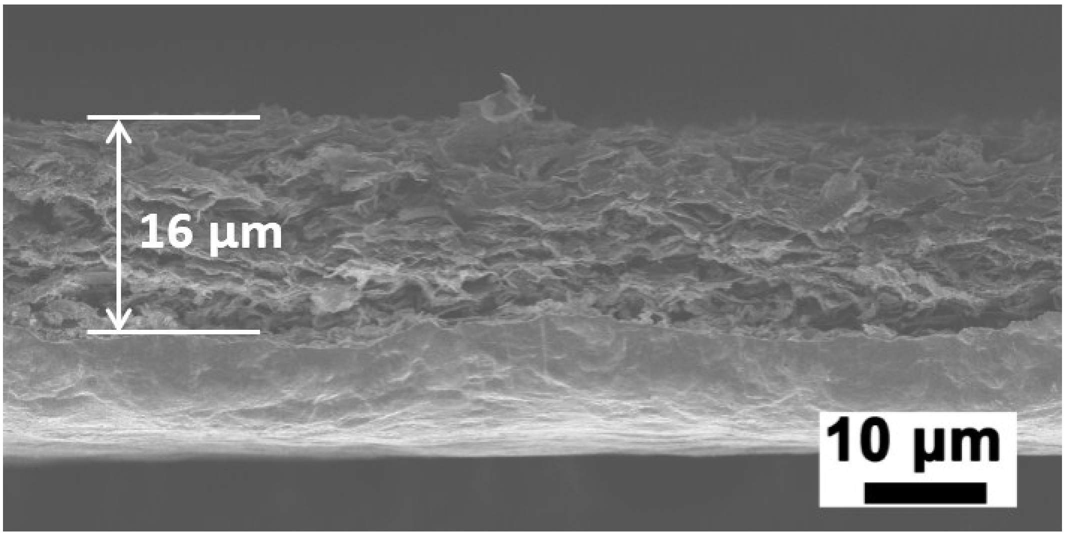

Fig. S1 Cross-section SEM images of CNS electrode.

As shown in Fig. S1, the thickness of the CNS electrode is ca. 16 μm.

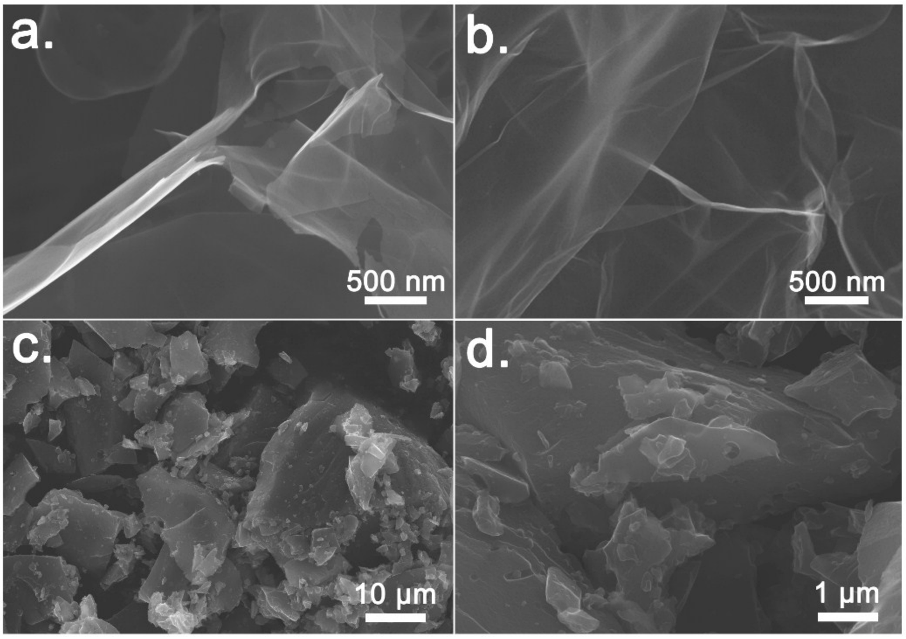

Fig. S2 SEM images of (a) CNS-2, (b) CNS-5 and (c, d) CM.

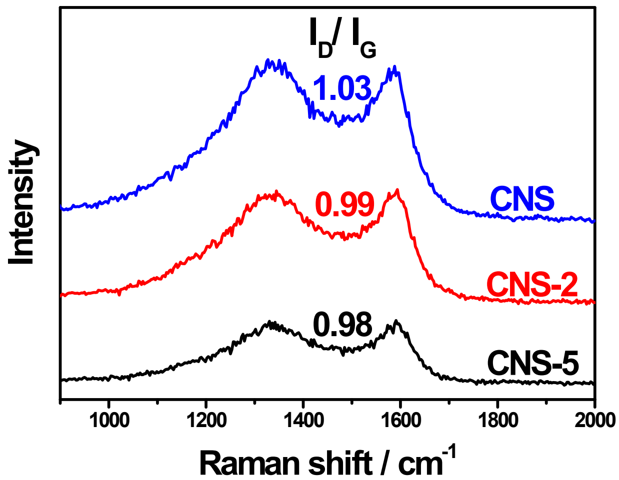

Fig. S3 Raman spectra of CNS, CNS-2 and CNS-5.

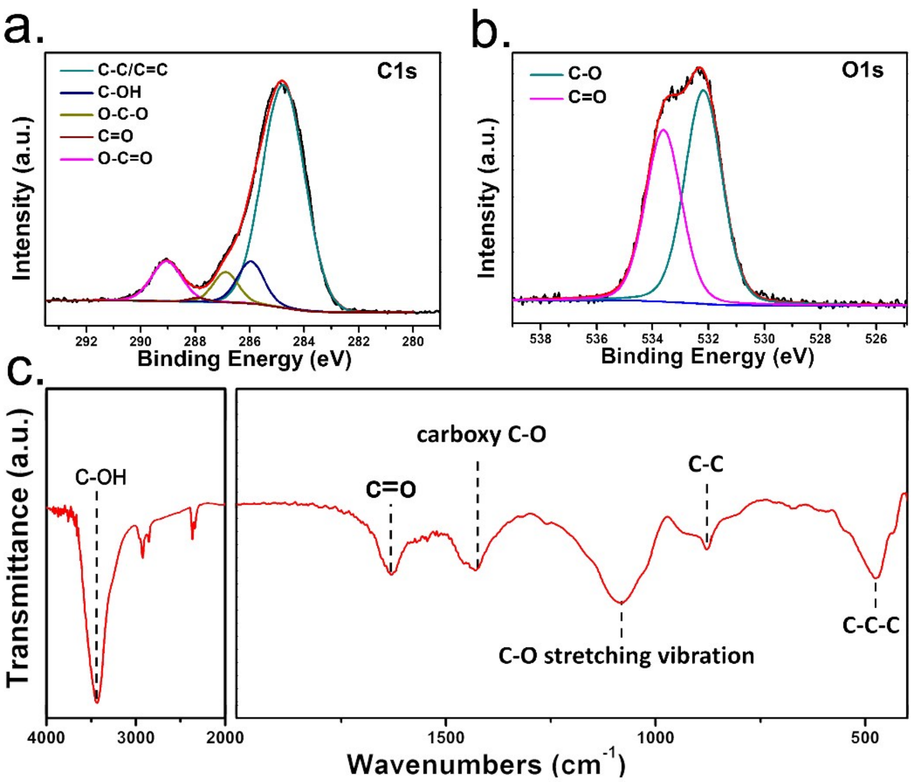

Fig. S4 High-resolution XPS spectra of (a) C1s and (b) O1s of CNS. (c) FT-IR pattern of CNS.

Table S1 Specific surface areas and pore parameters of CNS measured by BET method.

Sample	SSA (m^2 g^{-1})	S_{mic} (m^2 g^{-1})	S_{mes} (m^2 g^{-1})	V_t (cm^3 g^{-1})	V_{mic} (cm^3 g^{-1})	V_{mes} (cm^3 g^{-1})
CNS	402.9	124.0	279.0	0.686	0.065	0.610

SSA: BET surface area. S_{mic}: t-Plot micropore area. S_{mes}: t-Plot mesopore area. V_{mic}: t-Plot micropore volume. V_{mec}: mesopore volume calculated by BJH method. V_t: total pore volume.

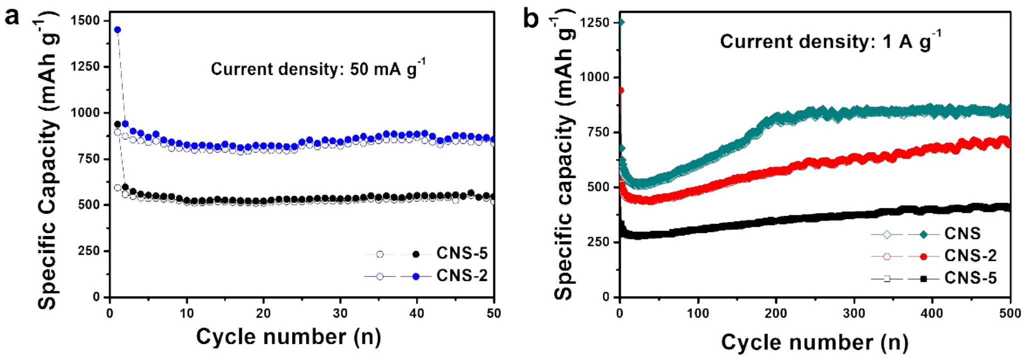

Fig. S5 Galvanostatic charge/discharge performance of the products at the current densities of (a) 50 mA g^{-1} and (b) 1 A g^{-1}.

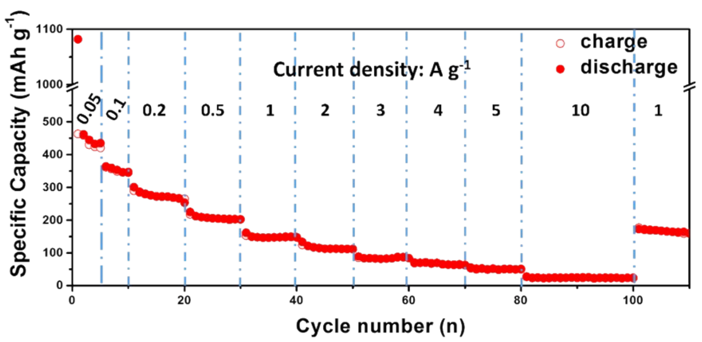

Fig. S6 Rate capabilities of CM anodes for LIBs at the current densities of 0.05, 0.1, 0.2, 0.5, 1, 2, 3, 4, 5, and 10 A g^{-1}, respectively.

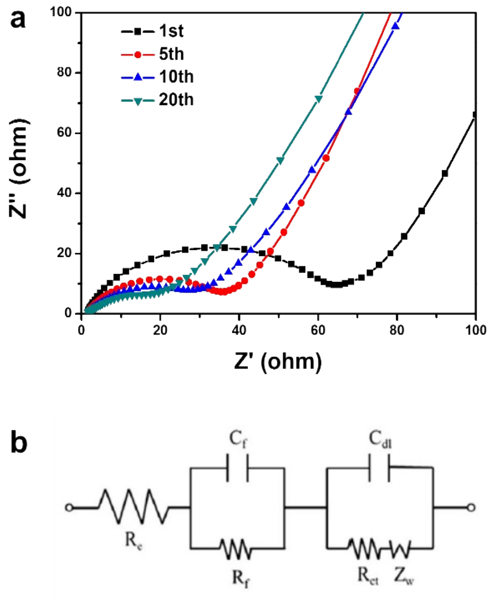

Fig. S7 (a) AC impedance spectra of CNS electrode at different cycles, (b) Randles equivalent circuit for CNS electrode.

Table S2. Kinetic parameters of CNS electrodes in LIBs at the voltage of 2.2 V after different cycles.

CNS	**R_{ct} (Ω)**	**R_e (Ω)**	**R_f (Ω)**	**C_f (F)**	**C_{dl} (F)**
1st	43.98	1.852	7.588	2.57E-06	4.28E-06
5th	21.17	1.787	4.431	3.33E-06	8.10E-06
10th	13.86	2.011	3.501	3.48E-06	1.26E-05
20th	7.036	1.672	2.252	4.30E-06	1.79E-05

R_{ct}: charge-transfer resistance; R_e: electrolyte resistance; R_f: contact resistance of SEI film on the surface of electrodes; C_f: capacitance of the solid-state interface layer at the surface of electrodes; C_{dl}: double-layer capacitance.

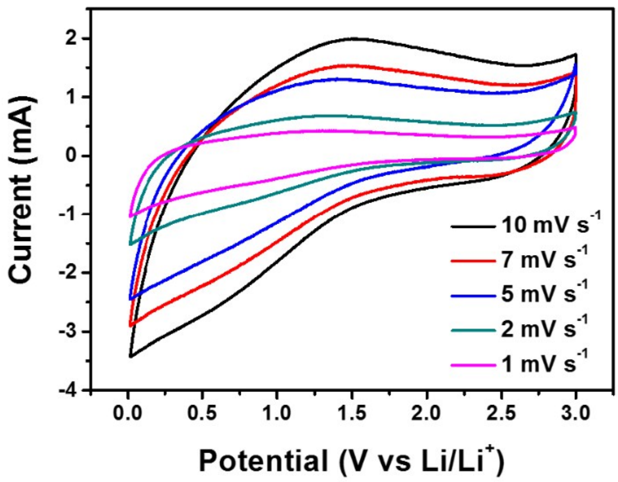

Fig. S8 CV curves of CNS at various scan rates from 1 to 10 mV s^{-1}.

To analyze contribution of capacitive and diffusion-controlled processes, the change of the current (i) along with the sweep rate (v) of cyclic voltammetry (CV) is investigated according to the following power law:[1-4]

$$i = av^b,$$

where i is the current, v is the scan rate, and a and b are adjustable parameters.

The contribution of these two processes can be separated quantitatively by the following equation:

$$i(v) = k_1 v + k_2 v^{1/2}$$

In this equation, $k_1 v$ represent the capacitive contribution, and $k_2 v^{1/2}$ represents the diffusion-controlled contribution.

And this equation can be rearranged to the equation as follows for easy analysis.

$$i(v)/v^{1/2} = k_1 v^{1/2} + k_2$$

Then k_1 and k_2 can be determined by fitting a straight line of $i(v)/v^{1/2}$ vs. $v^{1/2}$, in which k_1 is the slope and k_2 is the y-intercept. By determining k_1 and k_2, we can get the normalized contribution of diffusion-controlled effect (Figure S9) and capacitive effect (Figure S10) in different voltage zones.

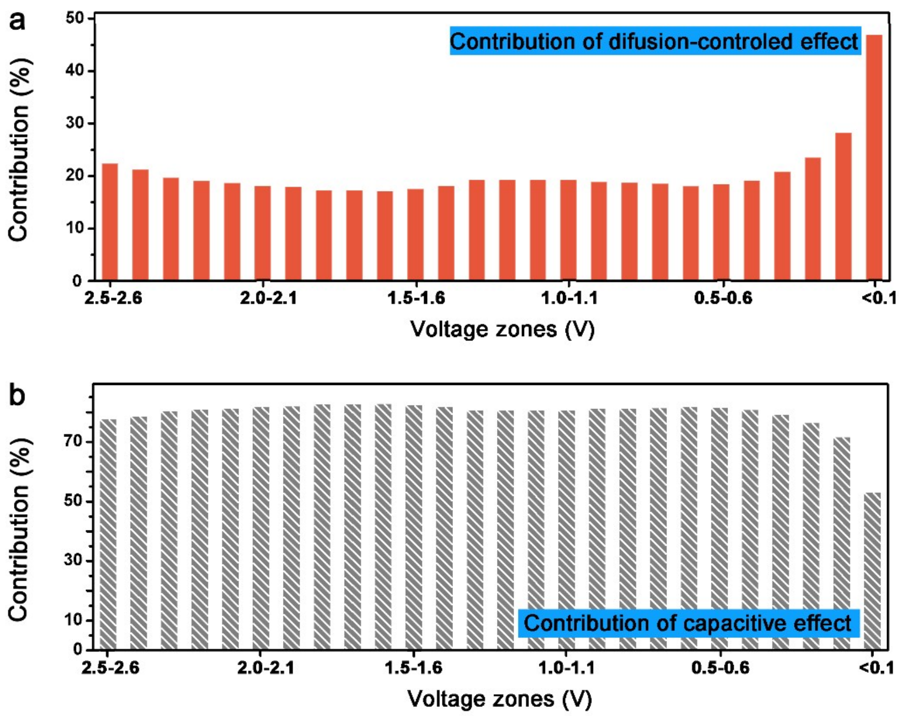

Fig. S9 Contribution of (a) diffusion-controlled effect and (b) capacitive effect of CNS electrode for LIBs in different voltage zones.

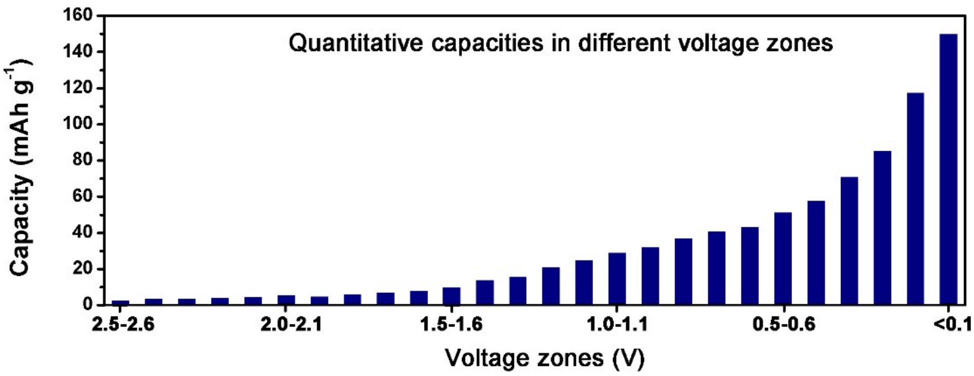

Fig. S10 Quantitative capacities of CNS electrode for LIBs in different voltage zones after 1000 cycles at 1 A g^{-1}.

We also calculated the quantitative capacities of CNS electrode after 1000 cycle at 1 A g^{-1} in different voltage zones. The results are shown in Fig. S10.

By combining the data of Fig. S9 and Fig. S10, we can get the quantitative diffusion-controlled capacities and capacitive capacities of CNS electrode for LIBs at 1 A g^{-1} after 1000 cycles in various voltage zones (**Fig. 4c**)

PCNS-0.5 with KCl as the template

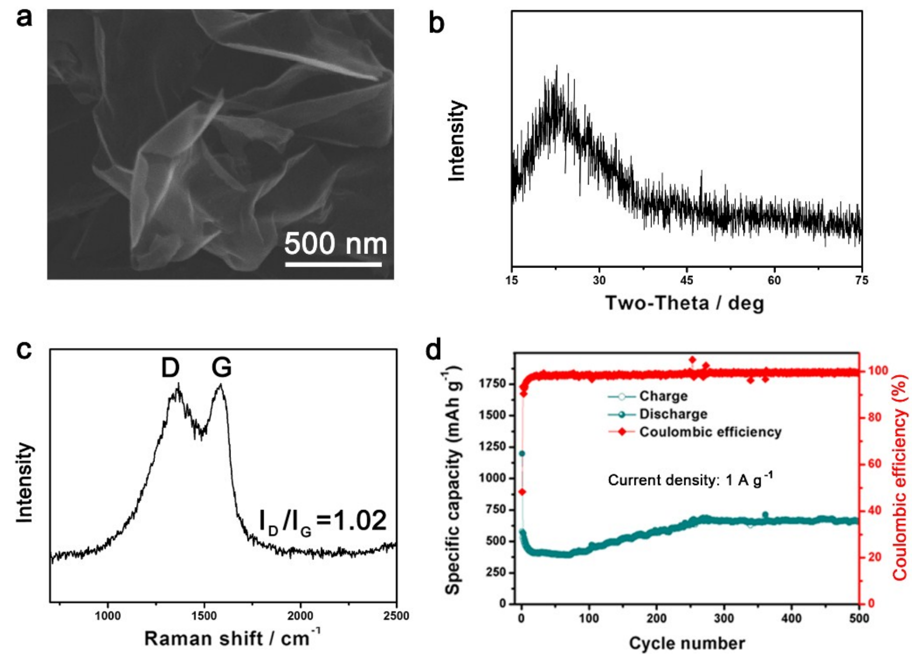

Fig. S11 (a) SEM image, (b) XRD pattern and (c) Raman spectrum of PCNS-0.5, (d) cycling performance of the PCNS-0.5 electrode at 1 A g^{-1} for LIBs.

As shown in Fig. S11a, PCNS-0.5 were micro-sized curled carbon nanosheets. XRD pattern and Raman spectrum of PCNS-0.5 indicate the similar amorphous carbon phase with that of CNS (Fig. S11b, c). Fig. S11d shows the cyclic performance of PCNS-0.5 electrode for LIBs at the current density of 1 A g^{-1}. PCNS-0.5 electrode shows the initial discharge and charge capacities of 1197.8 and 578.2 mAh g^{-1}, respectively, with an initial coulombic efficiency of 48.3%. And the reversible capacity stabilizes at ca. 670 mAh g^{-1} after 500 cycles.

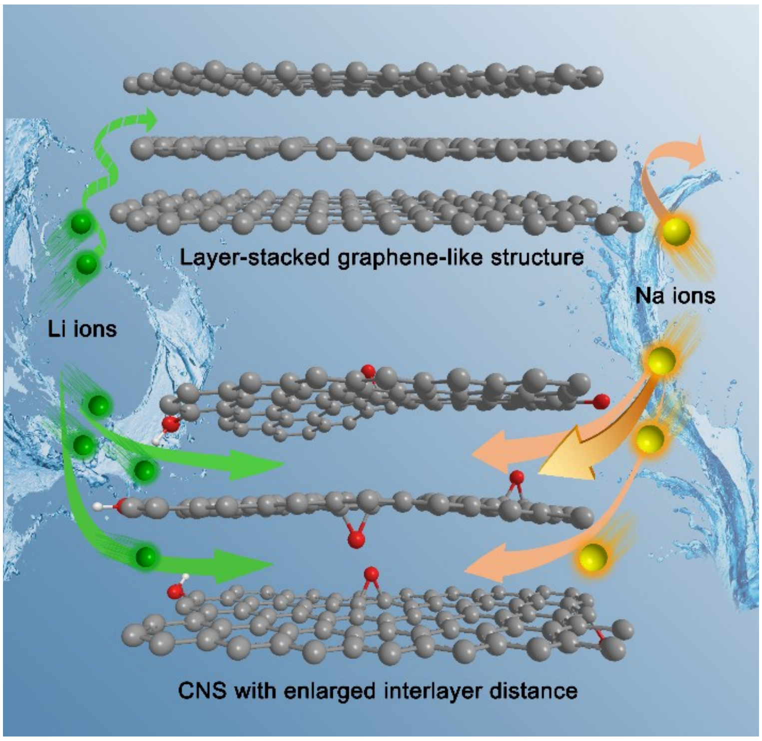

Fig. S12 Schematic illustration of Li/Na storage.

Reference

(1) Kim, H.; Hong, J.; Park, Y.-U.; Kim, J.; Hwang, I.; Kang, K. *Adv. Funct. Mater.* **2015**, *25*, 534.

(2) Wang, J.; Polleux, J.; Lim, J.; Dunn, B. *J. Phys. Chem. C* **2007**, *111*, 14925.

(3) Fu, L.; Tang, K.; Song, K.; van Aken, P. A.; Yu, Y.; Maier, J. *Nanoscale* **2014**, *6*, 1384.

(4) Augustyn, V.; Come, J.; Lowe, M. A.; Kim, J.; Taberna, P.-L.; Tolbert, S. H.; Abruña, H. D.; Simon, P.; Dunn, B. *Nature materials* **2013**, *12*, 518.